Sensors & Transducers, Vol. 247, Issue 8, December 2020, pp. 1-7

Sensors & Transducers
Published by IFSA Publishing, S. L., 2020
http://www.sensorsportal.com

Optical Phase Readout Instrument for Picometer-level Precision Heterodyne Interferometers

[1,*] J. J. Esteban Delgado, [3] A. Andersen, [1] I. Bykov, [1] D. Coutinho, [1] M. Dovale Alvarez, [1] G. Fernández Barranco, [2] O. Gerberding, [1] G. P. Guizzo, [3] A. Hornstrup, [3] N. C. Jessen, [4] M. Lieser, [1] P. Martínez Cano, [3] S. Møller Pedersen, [1] F. Öztürk, [1] D. Penkert, [1] A. Pizzella, [3] J. Raagaard Petersen, [1] J. Reiche, [3] K. Rommedahl, [1] T. Schwarze[1], [3] D. Tcherniak, [1] C. Vorndamme, [4] S. Wittig, [1] K. Yamamoto and [1] G. Heinzel

[1] Max Planck Institute for Gravitational Physics (Albert Einstein Institute) and Leibniz Universität Hannover, Institut für Gravitationsphysik, Callinstrasse 38, 30167 Hannover, Germany
[2] Universität Hamburg, Faculty of Mathematics, Informatics and Natural Sciences Physics Department, Institute for Experimental Physics, Luruper Chaussee 149, D-22761 Hamburg, Germany
[3] National Space Institute – DTU Space, Technical University of Denmark, Elektrovej, DK 2800 Kongens Lyngby, Denmark
[4] European Space Agency (ESA), European Space Research & Technology Centre (ESTEC), Keplerlaan 1, PO Box 299, NL-2200 AG Noordwijk, The Netherlands
[1] Tel.: +49 - (0) 511-762-17882
[*] E-mail: juan.jose.esteban@aei.mpg.de

Received: 9 November 2020 /Accepted: 15 December 2020 /Published: 31 December 2020

Abstract: A laser interferometer typically combines a number of beams that travel different optical paths to determine factors such as lengths, surface irregularities or the index of refraction of materials. Heterodyne detection is a well-established method for sensing tiny optical pathlength displacements through measurements of the phase shift between interfering signals. The ability of measuring displacements with high dynamic range and accuracy at the picometer-level has made this technique a crucial resource in many high-precision metrology applications, particularly for gravitational physics experiments in space, where one of the interfering beams is sensed at ultra-low light power. This article provides an overview of the design, construction and test facilities for an optical phase readout instrument able to extract picometer-stable displacement and nanometer-stable tilt measurements over thousands of seconds from a laser link operating at MHz heterodyne frequencies. The optical pathlength sensitivity of the instrument has been measured down to 1 pm/√Hz for frequencies above 3 mHz. The pitch and yaw pointing sensitivity is required below 5 nrad/√Hz and performed by applying the differential wavefront sensing technique. The instrument sensitivity seems to be limited above 3 mHz by ADC clock timing jitter and below 1 mHz by phase distortion caused by temperature fluctuations in the front-end electronics circuitry. Noise budgets and coupling mechanisms for both longitudinal and angular displacements are still under investigation with the design goal of an enhanced instrument performance with reasonable margins over the stringent sensitivity requirements.

Keywords: Gravitational physics, Optical metrology, Laser ranging, Phase-locked loop, Pseudoranges, Optical communication.

1. Introduction

Laser metrology based on heterodyne detection is a powerful method to monitor tiny optical pathlength displacements with high precision and large dynamic range. In contrast to non-coherent detection schemes, heterodyne interferometry leads to an achievable phase sensitivity at the sub-nanometer level, even when the received beam is detected at ultra-low light power levels [1-3]. A local oscillator (LO) signal is used as a stable reference and is combined with the measurement beam, translating the information of the received signal to the radio-frequency (RF) band, i.e., to a designed intermediate frequency that can be easily processed using standard electronics. The superposition of the two interfering beams is captured by a photoreceiver that generates a photocurrent replicating the phase of the measurement beam relative to the stable local reference beam. This technique enables the development of precise laser metrology systems through phase measurements of optical wavelengths (typically in the nanometer range), allowing the monitoring of relative displacements at even sub-picometer accuracy. Heterodyne laser interferometers have been employed with great success in spaced-based gravity and geodesy missions [4-8], which require high precision displacement sensors with a large dynamic range over laser links operated at picowatts of received optical power levels. This article provides an overview of the design, development and optical verification facilities for a phase readout system suitable for heterodyne laser interferometers with stringent performance requirements over time scales of thousands of seconds. In Section 2, the top-level requirements of the instrument are summarized. The hardware architecture is described in Section 3, and our next realization, currently under development, is described in Section 4. The test facilities for optical performance verification and the demonstration of pm-level stable interferometry is reported in Section 5, followed by the conclusions in Section 6.

2. Performance Goals and Requirements

In heterodyne interference, optical pathlength changes are translated into phase shifts of a sinusoidal signal, which are measured with a phasemeter [9]. Certain readout noise mechanisms can be mitigated by the use of suitable feedback systems. However, several fundamental noise sources exist that ultimately limit the readout noise performance of the instrument. Space-based gravitational-wave detection interferometers, aiming to reach a shot-noise-limited performance, provide some of the most stringent requirements to such phase readout instruments. The phasemeter has to operate and reach its design performance even when the measurement beam is extremely weak, resulting from the long propagation distance through the interferometer arms, the beam divergence, and the finite size of the receiving telescope [10]. The received optical signal power, typically in the order of 100 pW per quadrant photodetector, yields a quantum limit in the residual phase fluctuations sensed by the detector, corresponding to a displacement noise floor of about 5 pm/√Hz. To avoid excess noise, the phasemeter is subject to a sensitivity requirement corresponding to a displacement noise floor of 1 pm/√Hz, i.e., below the shot noise limit.

The high-sensitivity phase readout results from interfering the optical link beam with a stable local oscillator with an offset frequency of up to 25 MHz. Beyond such heterodyne frequency, electronic noise from the quadrant photoreceiver becomes the dominant noise contribution in the measurement chain [11]. To enable a stable heterodyne signal at the photoreceiver outputs, the instrument features a tunable offset phase locking scheme able to operate the laser link as an optical transponder. After conducting an autonomous beat note acquisition procedure [12-13], the phase readout of the heterodyne signal is used by the controller to mutually lock both interfering beams and return the local laser as a high power phase replica of the incoming light. It also allows compensating for Doppler effects while ensuring operation under environments with high diffraction losses, e.g., enabling measurements over larger distances in contrast to passive retroreflector configurations. The built-in optical transponder controllers have been designed for tracking frequency varying beat note signals in the range of up to a few Hz/s and able to operate under weak-light conditions.

The laser transponder scheme is designed to enable a stable heterodyne signal within the photoreceiver bandwidth. In order to achieve a displacement sensitivity of 1 pm/√Hz for beat notes up to 25 MHz, the necessary clock timing jitter stability between R_x/T_x remote terminals would need to be approximately 40 fs/√Hz [14]. Without a direct mechanism for timing synchronization between Rx/Tx instruments, the optical metrology system requires the realization of a clock noise removal scheme in order to subtract the excess phase noise that couples into the laser interferometer. To measure the relative clock noise contribution, a 10 MHz reference oscillator is multiplied by an integer factor (typically 240) and modulated as high-frequency (either 2.4 GHz or 2.401 GHz) phase modulation sidebands into each laser link by using approx. 10 % of the optical link power. After interference between local and incoming lasers, the phase measurement of the resulting sideband-to-sideband beat note contains the amplified clock noise information that is necessary to remove the clock noise in post-processing [15].

A desirable byproduct of the laser transponder configuration is that the metrology system features Doppler shift estimations between the Rx/Tx terminals by reading out the frequency of the interferometric signals, enabling precise measurements of both relative displacements and velocity between terminals. Relative measurements are combined with absolute position estimations by applying a second phase modulation scheme onto the laser link. The applied absolute ranging concept is inherited from Global Positioning Systems (GPS) by implementing a Direct-Sequence Spread Spectrum (DSSS) modulation scheme. In contrast to other ranging methods, this development provides a low-depth modulation index to reduce both the optical power allocated to the Pseudo-Random Noise (PRN) modulation and the residual carrier phase noise due to fast PRN transitions. Thus, this ranging scheme uses only approx. 1 % of the available optical link power and achieves sub-meter ranging accuracy for PRN chipping rates around 1 MHz, while most of the light power is used for precise heterodyne interferometry and gravitational wave astronomy [16-17]. This PRN ranging scheme determines the light travel time over the interferometric arm, so-called pseudorange measurements, due to the fact that clock differences between terminals are coupled into the measurement and therefore computed with an accuracy at the nano-second level, i.e., at the level of the absolute ranging accuracy. Thus, this optical metrology system overcomes one of the limiting factors of laser interferometers, the range ambiguity. Moreover, this DSSS modulation scheme enables optical communication between terminals by encoding PRN codes with data information running at lower bit rates. Experimental results have shown ranging measurements with centimeter rms noise at 3 Hz of updating rate and the viability of highly reliable data transfer at several kilobits per second under ultra-low light power (1 pW) conditions [17].

A major readout noise contribution of the phasemeter instruments has been identified as ADC timing jitter above 3 mHz. Compliance to the ADC timing jitter requirement is actually quite challenging and difficult to achieve for space-graded components. To achieve the required phase-fidelity of the instrument, the so-called “pilot tone correction”, a calibration technique is applied. A stable reference tone at a fixed frequency is superimposed onto each ADC input referred to the GHz clock sideband signals. By injecting the pilot tone with a high frequency, typically 75 MHz, the measured phase noise is attributed mainly to ADC time jitter. A single pilot tone is added to all ADC channels of a PMS instrument, such that after applying an appropriate calibration factor, the phase jitter can be effectively subtracted through the phase measurements of the pilot tone [18].

Temperature fluctuations in the measurement chain have been identified as a major limiting factor below 1 mHz, placing tight constraints on the thermal stability of the instrument. It is especially crucial at the signal conditioning electronics, prior to digital acquisition, and at the analog electronics for pilot tone frequency synthesis [18].

Table 1 summaries the performance goals of the phase readout instrument as well as the most relevant noise sources coupling into the readout scheme. The largest noise contribution to the phase readout stems from laser frequency noise (LFN) due to an unequal armlength configuration of the interferometric arms. LFN is ultimately suppressed on ground via a post-processing technique called time-delay interferometry (TDI) [19], which combines time-delayed versions of the raw phasemeter measurements to virtually synthesize an interferometer with equal armlengths, minimizing the presence of LFN to the required level. However, in flight, the phasemeter instrument operates under an excess LFN contribution with a dynamical range of 8 to 11 orders of magnitude above its equivalent phase noise sensitivity of 1 µcycle/√Hz, which corresponds to a 1 pm/√Hz displacement noise for a laser wavelength of 1064 nm.

3. Technology Demonstrator

The most critical functional and performance aspects of the phasemeter instrument have already been proven in hardware, supported by a technology development activity initiated by the European Space Agency (ESA) [20]. The photograph in Fig. 1 shows the hardware realization for the elegant breadboard demonstrator. It is characterized by a modular configuration, which enables parallel development and standalone testing of each individual module prior to integration. This development enables the phase readout of up to 24x independent channels. It features laser frequency control for up to 2 laser systems, and performs PRN phase modulation for pseudorange estimations and optical data transfer.

Fig. 1. Photograph of the elegant breadboard demonstrator.

This phasemeter instrument enables substantial signal processing capabilities based on its embedded real time processors, i.e., 8x FPGA cores with approximately 675k logic cells in total, as well as an ARM9 microprocessor with double-precision floating-point computing features.

Table 1. Performance goals and current best estimates for coupling into readout noise.

Parameter	Phase Measurement System
Number of readout channels	48 independent readout channels per instrument, with 16 channels in cold redundancy
Measurement band	100 µHz – 0.1 Hz
Heterodyne frequency range	5 – 25 MHz
Wavelength	1064 nm
Doppler shift change rate	20 Hz s^{-1}
Rx optical power levels (@ 1xQPR)	~100 pW for science readout ~10 pW for clock noise transfer ~ 1 pW for absolute ranging and data transfer
Shot noise level	~ 5 pm $Hz^{-1/2}$
Optical pathlength noise precision	1 pm $Hz^{-1/2}$
Laser phase noise level (@ 1Hz)	10^8 – 10^{11} µcycle $Hz^{-1/2}$ (frequency-dependent)
Equivalent phase noise precision	1 µcycle $Hz^{-1/2}$
Angular noise	5 nrad $Hz^{-1/2}$ (Differential Wavefront Sensing)
Timing noise	40 fs/√Hz for 25 MHz heterodyne signals
Equivalent ADC phase noise	18 µrad/√Hz for 75 MHz pilot tone
Ranging accuracy (@ 1Hz)	Sub-meter precision/sub-nanoseconds timing resolution
Thermal stability (@1 mHz)	0.1 K $Hz^{-1/2}$
Nominal Carrier to Noise Density	> 70 dBHz single phase readout channel
Beat note acquisition	Required (FFT-based algorithm 8192 points at 80 MHz and 10 MHz/s frequency sweeping for laser frequency scanning)
Laser offset phase locking	Required (typ 10 kHz loop bandwidth)
Multi-tone tracking	Required (based on digital phase locked loop running at 80 MSPS)
AC amplitude readout	Required (12-14 bit resolution)
DC amplitude readout precision	Required (24 bit resolution)
Clock sideband synthesis	Configurable either 2.4 GHz or 2.401 GHz
PRN chipping rate	1 MHz with 1024 code length
Optical data rate	20 kbps – 60 kbps
Configurable output data rate	1 Hz – 100 Hz for science readout (incl optical readout for drag-free attitude control) 1 Hz – 10 kHz for FFT readout (diagnostics and beat note acquisition phases) 1 Hz for telemetry

The microprocessor performs the filtering of scientific data and enables output data transfer via both Ethernet and USB interfaces. This metrology system was used to successfully verify full functional and performance requirements under a thermally controlled environment with 0.1 K/√Hz temperature stability at 1 mHz. Our next realization, currently under development, aims to demonstrate performance in space environments and to upgrade the technology readiness level for all crucial parts.

4. Next Development Status

A technical challenge for upgrading our phasemeter instrument is that it shall maintain both a high phase fidelity and thermal stability performance in vacuum conditions while demanding a high signal processing capability and power consumption. Therefore, an adequate thermo-mechanical design is critical for its development. Fig. 2 shows an illustration of the current baseline of the instrument, including the mechanical structure housing the electronics, which features several thermal management strategies that have been implemented following extensive thermal modelling of the instrument using the finite element method. The initial modular architecture has been re-structured into four different modules:

- 4x Back End Electronics (BEE) Modules for signal conditioning electronics and digital core signal processing, featuring a total capability of 48x readout channels.
- 1x Frequency Distribution Module (FDM), generating all internal frequencies as needed by the PMS instrument and referred to an external ultra-stable oscillator (10 MHz reference) as well as synthesis of GHz clock sideband signals for phase modulation.
- 1x Data handling and Laser Control (DHLC) for external communication, laser frequency control and PRN phase modulation.
- 1x Power Supply Module (PSM) for power supply and internal distribution, including an external power bus line for supplying QPR bias voltages and their front-end electronics.

To consolidate the feasibility of a passive thermo-mechanical design and to minimize the thermal coupling into phase noise performance, the construction of a demonstration model is currently under development as part of the design phase. As shown in Fig. 3 and Fig. 4, this early prototyping already started, allowing us to break down the complexity of the final realization into two parts:

1. Demonstration model for the verification of the thermo-mechanical design and consolidation of key software modules for early functional and performance testing in vacuum conditions.
2. Engineering model for electronics, software and interface re-work by replacing commercial off-the-shelf components by space-graded equivalent parts.

Fig. 2. Illustration of the thermo-mechanical enclosure for the next generation of the phasemeter instrument.

Fig. 3. Illustration of a prototype for the Back-End Electronics Module currently under manufacturing.

Fig. 4. Illustration of a prototype for the Frequency Distribution Module currently under manufacturing.

Both developments shall be verified in thermal vacuum conditions. Fig. 5 and Table 2 show our test facilities and the main features for thermal cycling tests at the unit level in compliance with the environmental tests requirements as specified by space projects.

Fig. 5. Photograph of the thermal vacuum chamber for functional and performance tests verification of the phasemeter instrument.

Table 2. Key features of the thermal vacuum chamber test facilities.

Parameter	Thermal Vacuum Chamber
Volume and Size	Cylindrical 2.6 m^3, Size 1400 × 1500 mm
Quality	< 10^{-6} mbar (time to reach vacuum 3 h)
Thermal control range	-65°C to +125°C
dT/dt	0.5°C per min
Homogeneity	< 1°C
Baseplate flatness	±0.1 mm/m
Baseplate material	Aluminum
ΔT shroud/baseplate	Up to 20°C
4x Optical windows	λ ~ 1064 nm (nominal)
4x Sub-D interfaces	37-Pin Sub-D
20x SMA interfaces	Double ended and floating shield

5. Experimental Performance Verification

A ground reference model of an ultra-stable optical bench was built by applying the same bonding techniques as used for space-based gravitational wave detectors [21]. Fig. 6 shows a photograph of the testbed, which features two separate instruments: the telescope simulator is the upper platform, and provides the optical bench (lower platform) with a measurement beam that can tilt with respect to a fixed point on the bench, so as to simulate test mass or spacecraft angular misalignments. The testbed can operate in two different configurations: one simulating the beam received from a remote spacecraft (i.e., a beam with flat intensity and phase profiles that is clipped and imaged onto the bench by the receiving telescope), and another simulating the beam reflected of a local test mass (i.e., a regular Gaussian beam) [22]. In both configurations the testbed is capable of reaching a displacement noise floor at the picometer level. The testbed has been used previously to demonstrate the performance of using imaging systems for passive optical suppression of tilt-to-length coupling (TTL). Currently, this ground reference model is being upgraded, conditioning the optical signals to conduct testing of the angular readout noise performance for the phasemeter instrument with a design goal of 5 nrad/√Hz in the observation band [23].

Fig. 6. Photograph of the ground reference model.

To experimentally verify the stringent phase noise performance over a high dynamic range without the loss of linearity, a three-signal test bed has been conducted, which linearly combines heterodyne signals from three different light sources. Fig. 7 shows a photograph of this quasi-monolithic test bed. As shown in Fig. 8, experimental results demonstrated picometer-level stable interferometry for the three beat signal recombination (red plot). The noise floor of the test bed facility can be found in the π pretests (green plot), suggesting sufficient stability [24]. This optical ground support equipment enables investigations in enhanced algorithms for both beat note acquisition procedures and laser phase locking as crucial aspects of the phasemeter instrument, even at weak-light conditions. Currently this verification platform is being upgrading to extend the experiment setup for testing the timing correction scheme in post-processing via Kalman-Filtering [25] and clock noise cancellation via TDI post-processing techniques [15].

Fig. 7. Photograph of the optical ground support equipment for testing key performance aspects of the phasemeter instrument.

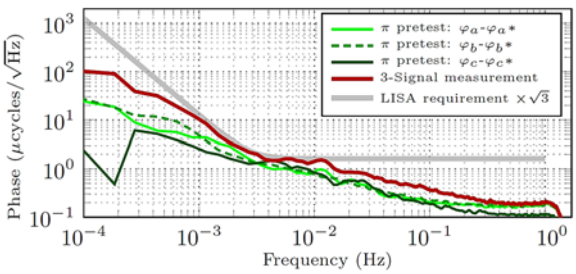

Fig. 8. Phase noise performance measurement of the elegant breadboard.

6. Conclusions

The optical metrology system described herein combines precision laser interferometry with low-depth modulation techniques to provide both picometer-level interferometry and absolute ranging measurements with optical communication capabilities in a single optical readout instrument. This optical metrology system overcomes one of the limiting factors on laser interferometers, the ambiguity range, as needed for laser frequency noise suppression in post-processing. Moreover, this scheme enables precise timing of readout data, indirect clock synchronization between remote terminals, Doppler estimations and optical acceleration measurements, being a versatile and attractive technology for several optical applications apart from our main research field, i.e., gravitational physics and geodesy.

A technology demonstrator was built and tested, fulfilling all critical functional and performance requirements of the instrument, and showing the feasibility of the optical metrology concept. The most challenging requirement, picometer-level phase stability over time scales of thousands of seconds, was optically demonstrated in an ultra-stable test bed even in the present of high dynamical ranges overpassing the phase sensitivity of the instrument by several order of magnitude due to the residual laser frequency noise coupling into the laser interferometers.

Acknowledgements

The authors greatly acknowledge the support of the German Space Agency, DLR (FKZ 50OQ1801) and the European Space Agency, ESA (RFQ /3-15545/18 /NL/BW).

References

[1]. P. McNamara, Weak-light phase locking for LISA, *Classical and Quantum Gravity*, Vol. 22, Issue 10, 2004, pp. S243-S247.

[2]. S. P. Francis, *et al.*, Weak-light phase tracking with a low cycle slip rate, *Optics Letter*, Vol. 39, Issue 18, 2014, pp. 5251-5254.

[3]. A. Liao, *et al*., Pico-Watt and Femto-Watt Weak-Light Phase Locking, *Int J Mod Phys D*, Vol. 11, Issue 7, 2002, pp. 1075-1085.

[4]. K. Abich, *et al*., In-Orbit Performance of the GRACE Follow-on Laser Ranging Interferometer, *Phys. Rev. Lett.,* Vol. 123, Issue 3, 2019.

[5]. M. Armano, *et al*., Sub-Femto-g Free Fall for Space-Based Gravitational Wave Observatories: LISA Pathfinder Results, *Phys. Rev. Lett*., Vol 116, Issue 23, 2016, 231101.

[6]. K. Danzmann, LISA and its pathfinder, *Nature Physics*, Vol. 11, 2015, pp. 613-615.

[7]. D. Castelvecchi, Success of gravity-wave satellite paves way for three-craft mission, *Nature News Physics*, Vol. 546, Issue 7660, 2017, pp. 583-584.

[8]. G. Wanner, Space-based gravitational wave detection and how LISA Pathfinder successfully paved the way, *Nature Physics*, Vol. 15, 2019, pp. 200-202.

[9]. O. Geberding, *et al*., Phasemeter core for intersatellite laser heterodyne interferometry: modelling, simulations and experiments, *Classical and Quantum Gravity*, Vol. 30, Issue 23, 2013.

[10]. LISA Mission L3 Proposal.

[11]. G. Fernández Barranco, *et al*., A Low-Power, Low-Noise 37-MHz Photoreceiver for Intersatellite Laser Interferometers using discrete heterojunction bipolar transistors, *IEEE Sensors Journal*, Vol. 18, Issue 18, 2018, pp. 7414-7420.

[12]. F. Cirillo, *et al*., Control system design for the constellation acquisition phase of the LISA mission, *J. Phys. Conf. Ser*, Vol 154, 2008.

[13]. D. Wuchenich, *et al.,* Laser link acquisition demonstration for the GRACE Follow-On mission, *Optics Express*, Vol. 22, Issue 9, 2014, pp. 11351-11366.

[14]. G. Heinzel, *et al*., Auxiliary functions of the LISA Laser link: ranging, clock noise transfer and data communication, *Classical and Quantum Gravity*, Vol. 28, Issue 9, 2011.

[15]. M. Tinto, *et al*., Time-delay interferometry and clock-noise calibration, *Phys. Rev. D*, Vol. 98, 2018, 042003.

[16]. A. Sutton, *et al*., Laser Ranging and communications for LISA, *Optics Express*, Vol. 18, Issue 20, 2010, pp. 20759-20773.

[17]. J. J. Esteban Delgado, *et al*., Experimental demonstration of weak-light laser ranging and data communication for LISA, *Optics Express*, Vol. 19, Issue 17, 2011, pp. 15937-15946.

[18]. Geberding O., *et al*., Readout for intersatellite laser interferometry: Measuring low frequency phase fluctuations of high-frequency signals with microradian precision, *Review of Scientific Instruments*, Vol. 86, Issue 7, 2015, 074501.

[19]. G. de Vine, *et al*., Experimental Demonstration of Time-Delay Interferometry for the Laser Interferometer Space Antenna, *Phys. Rev. Lett*., Vol. 104, Issue 21, 2010, 211103.

[20]. S. Barke, *et al*., LISA Metrology System, Link.

[21]. M Chwalla, *et al*., Design and construction of an optical test bed for LISA imaging systems and tilt-to-length coupling, *Class. Quantum Grav*., Vol. 33, Issue 24, 2016, 245015.

[22]. M Chwalla, *et al*., Optical Suppression of Tilt-to-Length Coupling in the LISA Long-Arm Interferometer, *Phys. Rev. Applied*, Vol. 14, Issue 21, 2020, 014030.

[23]. G. Heinzel, *et al*., Tracking-Length and Differential-Wave-Front-Sensing Signals from Quadrant Photodiodes in Heterodyne Interferometers with Digital Phase-Locked Loop Readout, *Physical Review Applied*, Vol. 14, 2020, 054013.

[24]. T. S. Schwarze, *et al*., Picometer-Stable Hexagonal Optical Bench to Verify LISA Phase Extraction Linearity and Precision, *Physical Review Letter*., Vol. 122, Issue 8, 2019, 081104.

[25]. Y. Wang, *et al*., First stage of LISA data processing. II. Alternative filtering dynamic models for LISA, *Phys. Rev. D*, Vol. 92, 2015, 044037.